Carbohydrate Polymers 86 (2011) 652–658

Contents lists available at ScienceDirect

Carbohydrate Polymers

journal homepage: www.elsevier.com/locate/carbpol

Nanostabilization of thermally processed high amylose hydroxylpropylated starch films

Katherine M. Dean[a,*], Eustathios Petinakis[a], Liz Goodall[a], Tony Miller[b], Long Yu[a], Natasha Wright[a]

[a] CSIRO Materials Science and Engineering, Gate 5 Normanby Rd, Clayton 3168, Australia
[b] CSIRO Mathematical and Information Sciences, Gate 5 Normanby Rd, Clayton 3168, Australia

ARTICLE INFO

Article history:
Received 13 January 2011
Received in revised form 30 March 2011
Accepted 3 May 2011
Available online 10 May 2011

Keywords:
Starch
Nanocomposites
Crystallinity
Hydroxypropylation

ABSTRACT

High amylose hydroxypropylated starch films have been formed using traditional extrusion technology with a range of plasticisers and nanosilicate additives such as montmorillonite. After thermal processing, these materials are predominantly amorphous, however under controlled humidity over time the evolution of B-type (found in high amylose starches) and Vh type (generally induced via processing) crystallinity was observed. These structural changes have been analysed and correlated to final mechanical properties (modulus, tensile strength and break elongation). A "nanostabilization" effect was also observed over time in starch samples containing montmorillonite. It is proposed that in these systems the montmorillonite disrupts the retrogradation process reducing the rate of embrittlement over time. This is of significant importance for improving the shelf life of thermoplastic starches for industrial applications.

1. Introduction

Human induced climate change, waste minimisation, rising commodity and energy prices are key drivers for science and technology aimed at finding sustainable long-term environmental solutions. The development of biodegradable polymers from renewable resources may offer a solution. One readily available biodegradable polymer is starch, however there are still many issues surrounding the processing and long term stability of starches for industrial type applications and replacement of conventional polymers.

Produced in plants, the structures of starches have been extensively studied and are a mixture of linear amylose (poly-α-1,4-D-glucopyranoside) and branched amylopectin (poly-α-1,4-D-glucopyranoside and α-1,6-D-glucopyranoside). The ratio of amylose (with a M_w of several hundred thousand) to amylopectin (with a M_w of millions) varies with the source. Amylose is the minor component (approximately 20–30%) of the starches (Buléon, Colonna, Planchot, & Ball, 1998; Kaur, Singh, & Singh, 2004). Amylopectin consists of highly branched chains, the short branching chains of amylopectin are partially in the form of double helices in clusters and are responsible for the crystalline properties of the starches (Buléon et al., 1998).

Many types of granular starch have been processed using conventional extrusion technology to produce thermoplastic (gelatinised) starch typically using a range of temperatures, extrusion conditions and chemistries (de Graaf, Karman, & Janssen, 2003; van Soest, Hulleman, de Wit, & Vliegenthart, 1996; Yu & Christie, 2001). During extrusion the starch granules are fragmented, hydrogen bond cleavage occurs between starch molecules (leading to loss of crystallinity) and partial depolymerisation of the starch molecule occurs (Poutanen & Forssell, 1996) High amylose content starches are generally more easily processed (van Soest et al., 1996).

There are typically two types of crystallinity in thermoplastic starches: residual crystallinity: native A- B- or C-type crystallinity caused by incomplete melting during processing and process induced crystallinity amylose V_H V_A or E_H type (van Soest et al., 1996).

One of the main issues with thermoplastic starches is retrogradation (recrystallization). The recrystallization of the amylose component is an irreversible and very fast process, the recrystallization of amylopectin is slower, and it is this component of crystallization with is generally referred to as retrogradation. This process is caused by the macromolecules forming hydrogen bonds under expulsion of water molecules or other solvents (de Graaf et al., 2003). Retrogradation causes shrinkage and embrittlement.

Starches are routinely modified to reduce their susceptibility to retrogradation from their hydrogen bonds by the formation of large side branches which can disrupt the process. The treatment of starch with propylene oxide – see Fig. 1, has been found to yield a material with much lower gelatinisation temperatures than native

* Corresponding author. Tel.: +61 395452686; fax: +61 395441128.
E-mail address: katherine.dean@csiro.au (K.M. Dean).

0144-8617/$ – see front matter
doi:10.1016/j.carbpol.2011.05.003

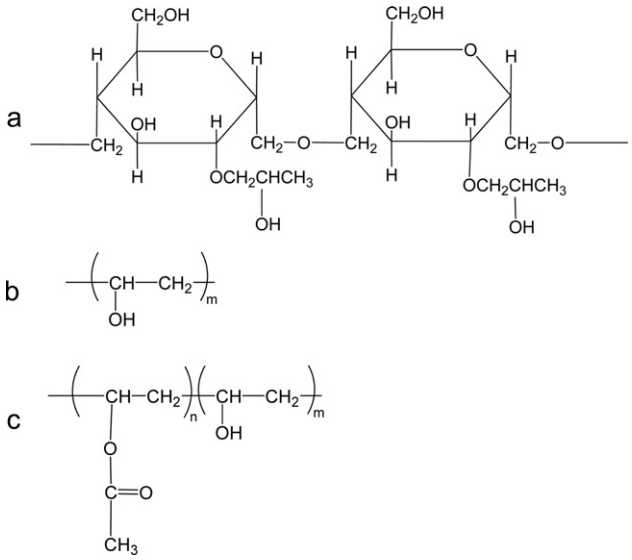

Fig. 1. Structures of (a) hydroxypropylated starch and (b) full and (c) partial hydrolysed PVOH.

starches (Kaur et al., 2004). These materials may also demonstrate reduced retrogradation, increased film clarity and flexibility, and improved water transmission properties (Kaur et al., 2004; Perera & Hoover, 1999). PVOH has also been used previously in extruded thermoplastic starch (Fishman, Coffin, Onwulata, & Willett, 2006; Follain, Joly, Dole, & Bliard, 2005; Mao, Imam, Gordon, Cinelli, & Chiellini, 2000) to improve properties such as processability (predominantly through improving melt flow properties) (Fishman et al., 2006; Mao et al., 2000) and elongation (Mao et al., 2000). Our group has recently studied thermoplastic starch nanocomposites with low loadings of PVOH (Dean, Do, Petinakis, & Yu, 2008) and others authors with high loadings of PVOH (Pascu, Popescu, & Vasile, 2008). In our recent work we investigated the key interactions between starch, polyvinyl alcohol and layered silicates and related structural changes (in particular order observed in the silicate structures using FTIR and XRD) to the overall mechanical performance of the materials (Dean et al., 2008).

Nanocomposite formation is another method to improve the properties of starch-based materials (including solvent cast, blended and extruded thermoplastic types) (Avella et al., 2005; Averous & Halley, 2009; Chen & Evans, 2005; Chivrac, Angellier-Coussy, Guillard, Pollet, & Averous, 2010; Chivrac, Pollet, & Averous, 2010; Chivrac, Pollet, Dole, & Averous, 2010; Dean, Yu, & Wu, 2007; Dean et al., 2008; Fischer, 2003; Huang, Yu, & Ma, 2004; Kalambur & Rizvi, 2004, 2005; Magalhães & Andrade, 2009; McGlashan & Halley, 2003; Park, Lee, Park, Cho, & Ha, 2003; Park et al., 2002; Wilhelm, Sierakowski, Souza, & Wypych, 2003a, 2003b; Zhang, Dean, & Burgar, 2010).

This paper demonstrates the property enhancements achieved in thermally processed hydroxypropylated starch nanocomposites (with addition of a third poly (vinyl alcohol) phase); and follows the evolution of crystallinity with relation to mechanical properties in these systems over time.

Table 1
Description of starch formulations utilised in extrusion.

Sample	Starch–H_2O (w/w)	PVOH (w/w)	MMT (w/w)
Starch	100		
Starch–GL	95	5	
Starch–NL	95	5	
Starch–MMT	95		5
Starch–MMT–GL	90	5	5
Starch–MMT–NL	90	5	5

2. Experimental

2.1. Experimental

A high amylose hydroxypropylated cornstarch (6.5% hydroxypropylation by weight – supplied by Penford – see Fig. 1a) was combined with 5 wt% of 2 types of poly(vinyl alcohol), a fully hydrolysed (M_w 22,000 g/mol – supplied by Gohsenol – see Fig. 1b) – NL and a partially hydrolysed (M_w 22,000 g/mol – supplied by Gohsenol – see Fig. 1c) – GL type together with an additional 20 wt% water. The clay used in this study was based on naturally occurring sodium montmorillonite clay (Cloisite Na+ – supplied by Southern Clay Products) – MMT.

The series of starch/PVOH/MMT/water formulations which were prepared for this study are shown in Table 1. The starch, PVOH and MMT formulations were firstly combined in a high speed mixer, water was added drop-wise whilst mixing at 500 rpm, once all water had been added, mixing continued at 1800 rpm for 5 min to ensure uniform dispersion of all components. In the second step

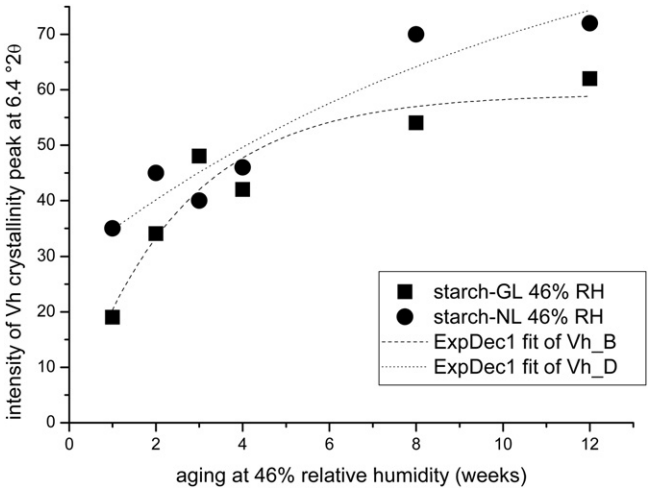

Fig. 2. Intensity of XRD peak at 6.4°2θ versus time for samples at 46% relative humidity (please note baseline starch did not exhibit a peak at this position).

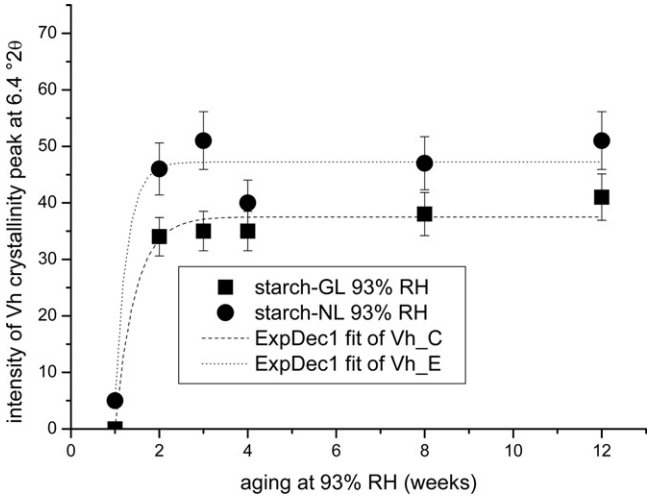

Fig. 3. Intensity of XRD peak at 6.4°2θ versus time for samples at 93% relative humidity (please note baseline starch did not exhibit a peak at this position).

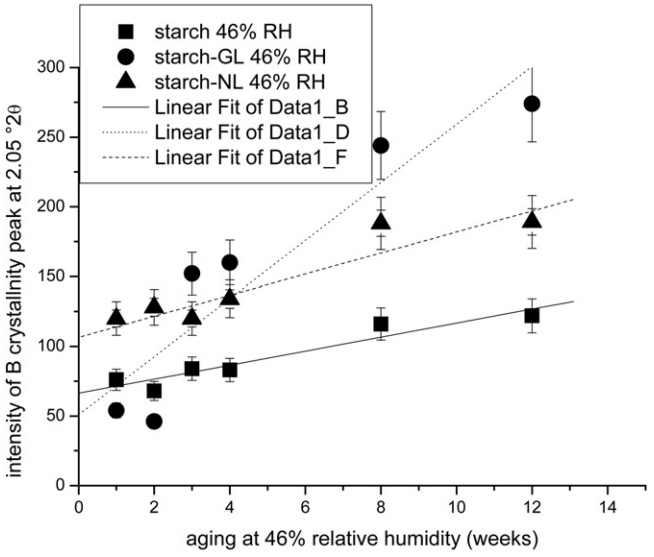

Fig. 4. Intensity of XRD peak at 2.05°2θ versus time for samples at 46% relative humidity.

a Theysohn co-rotating twin screw extruder, with diameter 30 mm and L/D 40, was used to process the starch nanocomposities using a low shear profile producing a melt temperature of 110 °C. The starch nanocomposite material was extruded directly into sheet form via a 0.5 mm die attached to the extruder. The extrusion of each formulation was duplicated to ensure reproducibility.

Dog-bone shaped samples were cut from the thermoplastic starch sheet immediately after extrusion. The first samples were tested 1 week after extrusion and the remaining 100 tensile bars of each formulation were placed in two humidity chambers, the first at 46% relative humidity (RH) and the 2nd at 93% RH, humidity was controlled using saturated salt solutions and continuously monitored over the time period of the experiment. Samples were removed periodically over a 3-month period and X-ray diffraction and mechanical property analysis undertaken.

Mechanical testing was undertaken as outlined in ASTM 638. A test speed of 10 mm/min was used and a minimum of 10 samples were tested for each formulation. Data is reported as the mean value of the 10 test specimens with the error bars representing plus or minus the standard error.

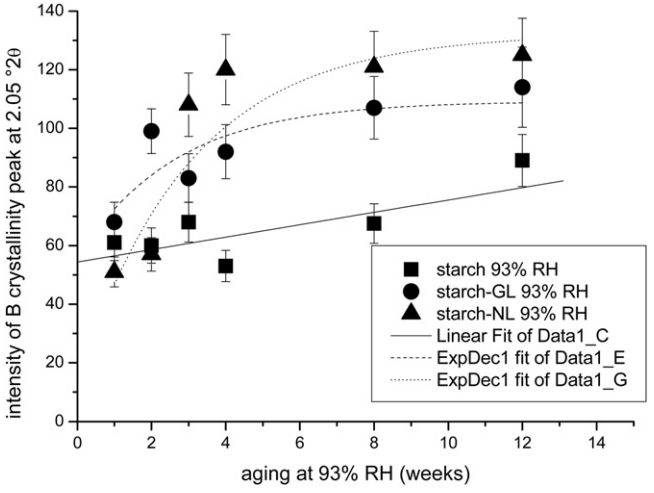

Fig. 5. Intensity of XRD peak at 2.05°2θ versus time for samples at 93% relative humidity.

Table 2
°2θ peak positions for A, B and Vh type crystallinity in starches.

A-type	B-type	Vh-type
14.8	2.5	7.1
16.6	5.5	12.6
17.7	10.8	19.4
22.6	14.8	22.1
26.3	17.0	
30.1	19.3	
33.2	22.1	
	23.8	
	26.1	
	30.9	
	34.0	

X-ray diffraction (XRD) was used to monitor the d_{001} spacing corresponding to the interlayer spacing of the clay and the crystalline structure of the starches. The XRD measurements were performed on the starch nanocomposite sheet samples using a Bruker D8 Diffractometer operating at 40 kV, 40 mA, Cu Kα radiation monochromatised with a graphite sample monochromator. A diffractogram was recorded between 2θ angles of 1° and 45°. Peak intensity was measured over time with the amorphous peak used as an internal standard.

The starch nanocomposites were imaged with a TEM using an accelerating voltage of 100 keV at magnifications of 25,000 times to study dispersions of clay particles. The samples were microtomed with a diamond knife directly from the extruded starch sheets at room temperature.

3. Results and discussion

Six different formulations of starch and starch nanocomposite were directly extruded into film – see Table 2 for formulations utilised. The film thicknesses from direct extrusion were maintained between 0.15 and 0.2 mm in an attempt to maintain similar ageing profiles throughout the samples. The addition of PVOH and MMT did improve the extrudability of the films and this is discussed in relation to the consistency of results obtained (in particular for the mechanical properties).

3.1. XRD analysis

3.1.1. Hydroxypropylated starch–PVOH

All films did remain predominantly amorphous over the 3-month ageing period. However, small amounts of different crys-

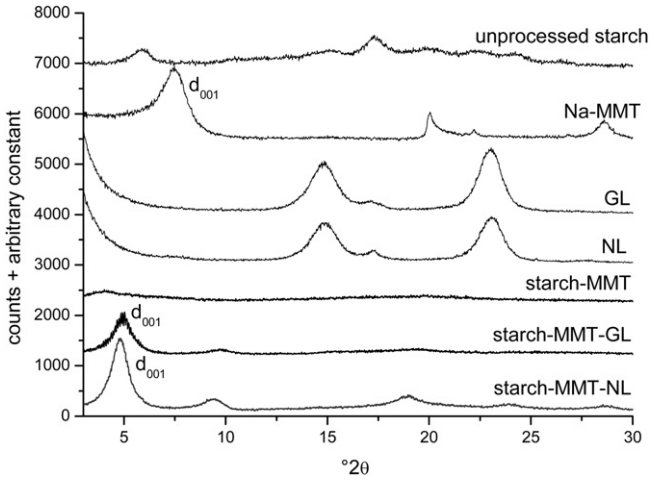

Fig. 6. XRD of unprocessed hydroxypropylated starch, neat Na-MMT, PVOH-GL, PVOH-NL and corresponding starch and starch–PVOH nanocomposite samples.

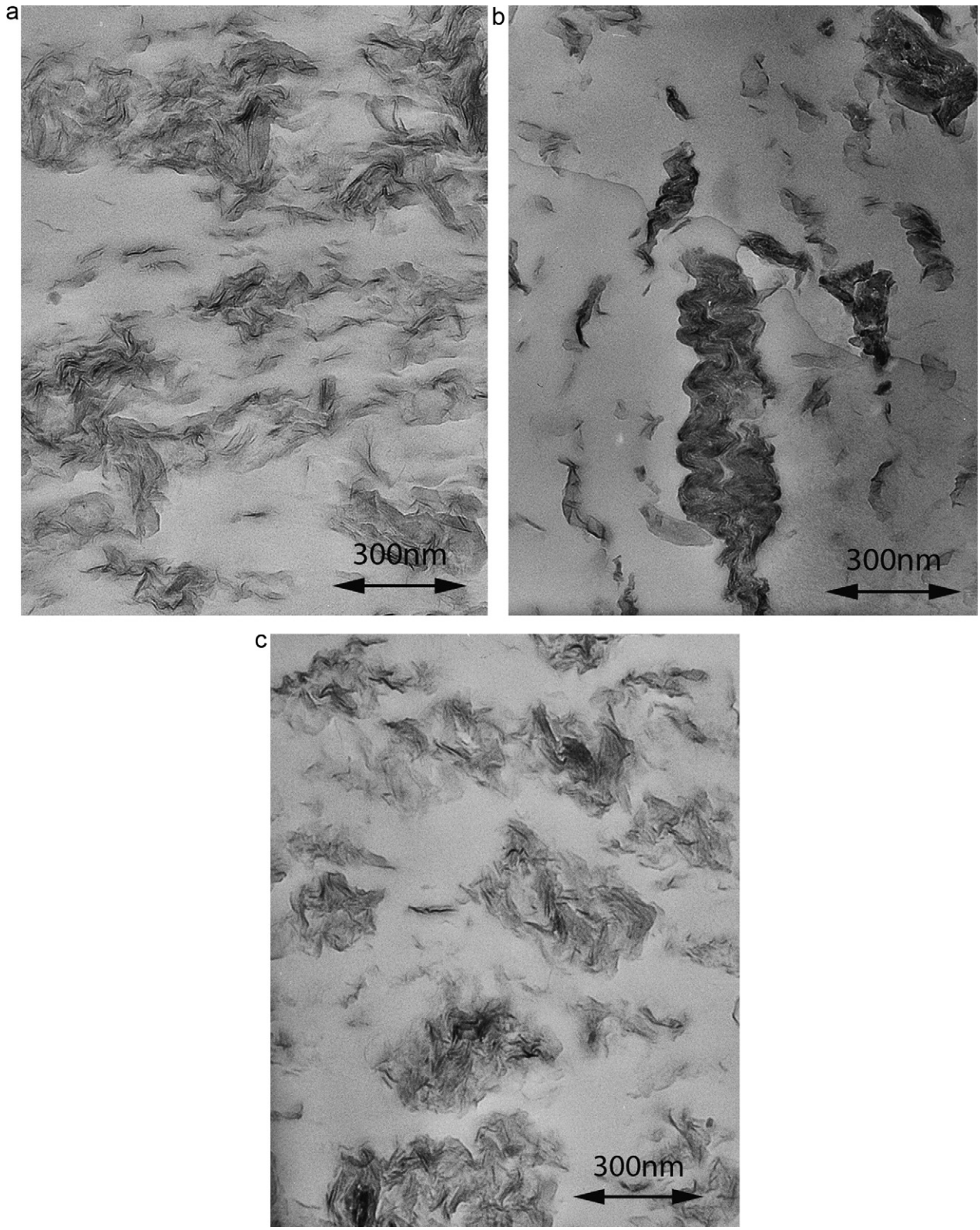

Fig. 7. TEM of (a) starch–MMT, (b) starch–MMT–GL and (c) starch–MMT–NL.

talline phases developed over ageing time at both 46% and 93% relative humidity, presumably as the polymer underwent retrogradation. The typical positions of the crystalline phases for A, B and Vh type crystallinity from the literature are shown in Table 2 (Le Bail et al., 1999; van Soest et al., 1996). The crystalline phases observed in the starch–PVOH systems were most likely B-type at 2.05°2θ and Vh-type at 6.4°2θ. Of particular interest is the novel formation of Vh type crystallinity normally due to amylose–lipid interactions which was only observed in the starch/PVOH samples (Le Bail et al., 1999; van Soest et al., 1996). It is proposed by the authors that the amylose–lipid and amylose–PVOH interactions may have been similar in crystallographic structure, thus the observation of the peak

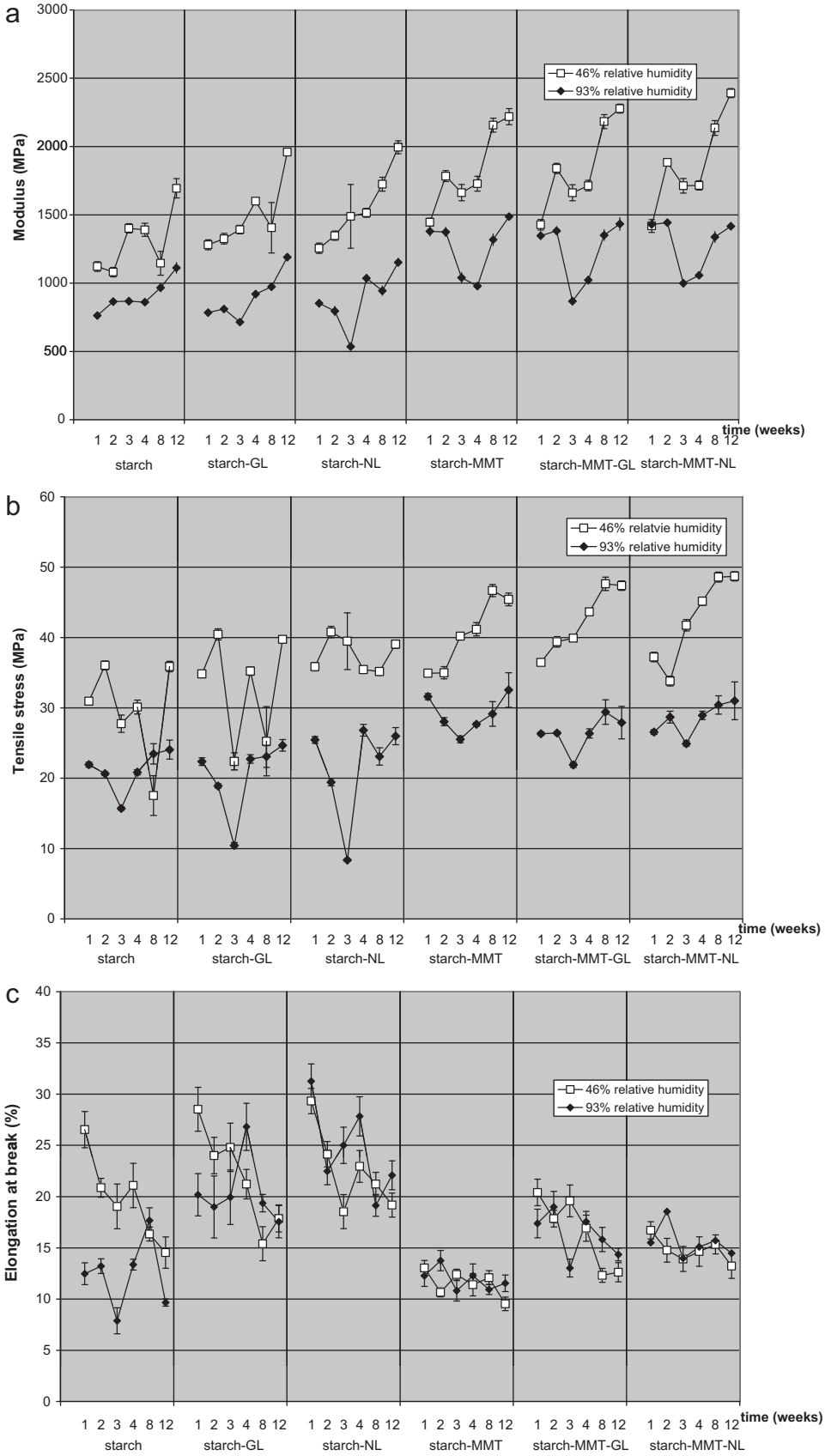

Fig. 8. (a) Modulus, (b) tensile stress (maximum) and (c) elongation at break (%) of samples versus ageing time (weeks 1, 2, 3, 4, 8, and 12) for each sample set.

at 6.4°2θ in samples containing PVOH comparable to Vh position due to amylose–lipid interactions (at 7.1°2θ) listed in Table 2.

The level of Vh crystallinity in the starch film containing fully hydrolysed PVOH (NL type) was the higher (based on peak height) than the partially hydrolysed PVOH (GL type). This may be explained by the presence of the bulky acetate grouping the partially hydrolysed system disrupting the crystallization process – see Figs. 2 and 3.

Addition of PVOH also led to greater amount of B crystallinity (particularly after 4 weeks) at both low and high humidity (see Figs. 4 and 5 respectively) as compared to the neat thermoplastic starch. It is assumed this peak is B-type as water is used as a plasticiser in our systems and the B type is typically described as a more loosely packed hexagonal assembly of the helices with a column of water molecules present in the centre of the hexagonal structure (van Soest et al., 1996). It is proposed that the PVOH could act as a plasticiser allowing more molecular movement and restructuring over time and thus observed as an increased level of crystallinity under these humidity conditions. After 3 months the intensity of B crystallinity (based on peak height) was greater at low humidity, this may have been due to a greater extent of retrogradation as the equilibrium moisture content was lower at the lower humidity and retrogradation is the process caused by expulsion of water molecules (de Graaf et al., 2003). Although the final level of B crystallinity was lower in the higher humidity condition, the initial rate of formation was higher possibly due to greater mobility.

3.1.2. Hydroxypropylated starch–PVOH–nanoclays

Although XRD analysis of the starch nanocomposites was undertaken at weeks 1, 2, 3, 4, 8 and 12, it was difficult to track any significant changes in crystal structure as many peaks of the starch are obscured by the more intense peaks of the montmorillonite – see Fig. 6.

Starch–MMT showed a clear (but broad and low intensity) peak at 10 Å corresponding to the d_{001} spacing of the clay. This indicated that most of the clay was probably exfoliated and that which remained in an ordered state was present in a number of different states (both tightly stacked and more loosely arranged). The starch–MMT–GL and starch–MMT–NL both had a much more ordered structure observed as a more intense sharp peak in the 17–18 Å region also corresponding to the d_{001} spacing – see Fig. 6. Our previous work has shown that PVOH molecules arrange in close proximity to the MMT and typically have a higher d spacing, this is observed in both partially hydrolysed and fully hydrolysed PVOH starch nanocomposite samples.

3.1.3. TEM analysis

Starch–MMT showed quite good dispersion of MMT platelets – see Fig. 7a. Both starch–MMT–GL and starch–MMT–NL (see Fig. 7b and c) showed more ordered structures and this correlated with what we observed in the XRD traces.

3.1.4. Mechanical properties

The modulus, tensile strength and elongation at yield for all samples at both 46% and 93% RH are shown in Fig. 8a–c. The measurement of mechanical properties at weeks 1, 2, 3, 4, 8 and 12 correspond to each data point moving left to right across the series of data.

Fig. 8a illustrates that the modulus of all three nanocomposites is higher than their precursors containing no MMT across both ageing profiles. Significant increases in modulus are commonly seen in conventional clay–polymer nanocomposites containing tactoids (due to the high intrinsic modulus of the clay) – often in sacrifice of tensile strength, elongation and toughness (LeBaron, Wang, & Pinnavaia, 1999). At 46% RH over time the modulus of both starch and starch–MMT systems increase as the samples lose moisture and become more brittle, this has been noted by others in conventional starch systems (Shogren, 1992). It may be noted that at higher humidity (93%) all starch nanocomposites and the starch samples containing PVOH show an initial drop in modulus (this is also shown to a lesser degree in the samples at lower humidity). This may be due to absorption of moisture to reach an equilibrium state which is promoted by both the MMT (this may be intergallery or edge hydroxyl interactions) and the PVOH (observed particularly in the more hydrophilic fully hydrolysed PVOH which does not contain residual acetate groups).

Fig. 8b shows the maximum tensile stress for the three nanocomposites increases over time for the 46% RH samples, the maximum tensile stress obtained is close to 50 MPa for the starch–MMT–NL sample. The maximum tensile stress for the three nanocomposites remains quite constant at the higher humidity as the materials are undergoing a process obtaining an equilibrium water content at that particular humidity in competition with changing crystallinity. The neat starch and starch PVOH samples do not show very clear trends in the maximum tensile strength, this may be explained by a number of means. Firstly the process to obtain similar film thickness to those produced in the nanocomposites reduced the consistency of the starch films; secondly the processes of water equilibration and system recrystallization were less hindered and could have led to more uncontrolled balance of these processes occurring during ageing.

The most significant figure to discuss in terms of evolution of mechanical properties is the stabilisation of the elongation at break for the nanocomposite samples at 46% RH – see Fig. 8c. A "nanostabilization" effect was observed over time in starch samples containing montmorillonite, with the starch–MMT and starch–MMT–NL samples maintaining a very constant break elongation over the 3-month period of testing. It is proposed that the montmorillonite disrupts the retrogradation process reducing the rate of embrittlement. The sample starch–MMT–NL at 46% RH shows both a stabilisation over time of elongation at break (close to 15% elongation maintained) predominantly due to the addition of nanoclays and a higher overall value of elongation predominantly due to the addition of the fully hydrolysed PVOH (NL type). The partially hydrolysed PVOH (GL type) produced slightly lower strains at break (particularly at high RH). This may have been due to the partially hydrolysed PVOH containing more hydrophobic acetate groups reducing the equilibrium water content of the film. Similar break elongation stabilisation effects are observed at higher humidity see Fig. 8c – however there is much more scatter in measurement for those samples not containing nanoclays, this variability is presumably due to the competing effects of sorption/desorption of water and retrogradation of the starch.

4. Conclusion

High amylose hydroxypropylated starch films have been formed using traditional extrusion technology using a range of plasticisers; with and without nano-additives. After thermal processing, these materials are predominantly amorphous, however under controlled humidity over time the evolution of B-type (found in high amylose starches) and Vh type (generally induced via processing) crystallinity was observed.

The level of Vh crystallinity in the starch film containing fully hydrolysed PVOH (NL type) was the higher than the partially hydrolysed version after 3 months. There was however a competing effect of the hydrophilic nature of the fully hydrolysed PVOH assisting in the maintenance of plasticiser (moisture) in the starch films led to slightly higher elongation at break (in both low and high humidity conditions). The lower level of Vh crystallinity observed in the partially hydrolysed PVOH (GL type) system may have been due

to the bulky acetate groups causing disruption of the crystallization process.

At low humidity (46%RH) a "nanostabilization" effect was also observed over time in starch samples containing montmorillonite, with the starch–MMT and starch–MMT–NL samples most clearly observed in the maintenance a very constant break elongation over the 3-month period of testing. It is proposed that the montmorillonite disrupts the retrogradation process reducing the rate of embrittlement. Similar stabilisation effects were observed at higher humidity however there was a little more variability in the data presumably due to the competing effects of sorption/desorption of water and retrogradation of the starch.

The sample starch–MMT–NL at both 46% and 93% RH shows both a stabilisation over time of elongation at break (close to 15% elongation) predominantly due to the addition of nanoclays and a higher overall value of elongation predominantly due to the addition of the fully hydrolysed PVOH (NL type).

Unfortunately due to the intensity and location of diffraction peaks from the montmorillonite the changes in crystallinity of the starch nanocomposites could not be fully visualised. Future work could involve using a different X-ray source to separate the diffraction peaks further. Future work could also involve using a lower percentage of MMT to maximise the absolute value of elongation at break whilst having the same stabilisation effect. Improving the break elongation and tensile strength stability over time is of significant importance for improving the shelf life of thermoplastic starches for industrial applications.

References

Avella, M., De Vlieger, J. J., Errico, M. E., Fischer, S., Vacca, P., & Volpe, M. G. (2005). Biodegradable starch/clay nanocomposite films for food packaging applications. *Food Chemistry*, *93*(3), 467–474.

Averous, L., & Halley, P. J. (2009). Biocomposites based on plasticized starch. *Biofuels Bioproducts & Biorefining-Biofpr*, *3*(3), 329–343.

Buléon, A., Colonna, P., Planchot, V., & Ball, S. (1998). Starch granules: Structure and biosynthesis. *International Journal of Biological Macromolecules*, *23*(2), 85–112.

Chen, B., & Evans, J. R. G. (2005). Thermoplastic starch–clay nanocomposites and their characteristics. *Carbohydrate Polymers*, *61*(4), 455–463.

Chivrac, F., Angellier-Coussy, H., Guillard, V., Pollet, E., & Averous, L. (2010). How does water diffuse in starch/montmorillonite nano-biocomposite materials? *Carbohydrate Polymers*, *82*(1), 128–135.

Chivrac, F., Pollet, E., & Averous, L. (2010). Shear induced clay organo-modification: Application to plasticized starch nano-biocomposites. *Polymers for Advanced Technologies*, *21*(8), 578–583.

Chivrac, F., Pollet, E., Dole, P., & Averous, L. (2010). Starch-based nano-biocomposites: Plasticizer impact on the montmorillonite exfoliation process. *Carbohydrate Polymers*, *79*(4), 941–947.

de Graaf, R. A., Karman, A. P., & Janssen, L. (2003). Material properties and glass transition temperatures of different thermoplastic starches after extrusion processing. *Starch - Stärke*, *55*(2), 80–86.

Dean, K., Yu, L., & Wu, D. Y. (2007). Preparation and characterization of melt-extruded thermoplastic starch/clay nanocomposites. *Composites Science and Technology*, *67*(3–4), 413–421.

Dean, K. M., Do, M. D., Petinakis, E., & Yu, L. (2008). Key interactions in biodegradable thermoplastic starch/poly(vinyl alcohol)/montmorillonite micro- and nanocomposites. *Composites Science and Technology*, *68*(6), 1453–1462.

Fischer, H. (2003). Polymer nanocomposites: From fundamental research to specific applications. *Materials Science and Engineering C*, *23*(6–8), 763–772.

Fishman, M. L., Coffin, D. R., Onwulata, C. I., & Willett, J. L. (2006). Two stage extrusion of plasticized pectin/poly(vinyl alcohol) blends. *Carbohydrate Polymers*, *65*(4), 421–429.

Follain, N., Joly, C., Dole, P., & Bliard, C. (2005). Properties of starch based blends. Part 2. Influence of poly vinyl alcohol addition and photocrosslinking on starch based materials mechanical properties. *Carbohydrate Polymers*, *60*(2), 185–192.

Huang, M. F., Yu, J. G., & Ma, X. F. (2004). Studies on the properties of montmorillonite-reinforced thermoplastic starch composites. *Polymer*, *45*(20), 7017–7023.

Kalambur, S. B., & Rizvi, S. S. H. (2004). Starch-based nanocomposites by reactive extrusion processing. *Polymer International*, *53*(10), 1413–1416.

Kalambur, S. B., & Rizvi, S. S. H. (2005). Biodegradable and functionally superior starch–polyester nanocomposites from reactive extrusion. *Journal of Applied Polymer Science*, *96*(4), 1072–1082.

Kaur, L., Singh, N., & Singh, J. (2004). Factors influencing the properties of hydroxypropylated potato starches. *Carbohydrate Polymers*, *55*(2), 211–223.

Le Bail, P., Bizot, H., Ollivon, M., Keller, G., Bourgaux, C., & Buléon, A. (1999). Monitoring the crystallization of amylose–lipid complexes during maize starch melting by synchrotron X-ray diffraction. *Biopolymers*, *50*(1), 99–110.

LeBaron, P. C., Wang, Z., & Pinnavaia, T. J. (1999). Polymer-layered silicate nanocomposites: An overview. *Applied Clay Science*, *15*(1–2), 11–29.

Magalhães, N. F., & Andrade, C. T. (2009). Thermoplastic corn starch/clay hybrids: Effect of clay type and content on physical properties. *Carbohydrate Polymers*, *75*(4), 712–718.

Mao, L., Imam, S., Gordon, S., Cinelli, P., & Chiellini, E. (2000). Extruded cornstarch–glycerol–polyvinyl alcohol blends: Mechanical properties, morphology, and biodegradability. *Journal of Polymers and the Environment*, *8*(4), 205–211.

McGlashan, S. A, & Halley, P. J. (2003). Preparation and characterisation of biodegradable starch-based nanocomposite materials. *Polymer International*, *52*(11), 1767–1773.

Park, H. M., Lee, W. K., Park, C. Y., Cho, W. J., & Ha, C. S. (2003). Environmentally friendly polymer hybrids. Part I. Mechanical, thermal, and barrier properties of thermoplastic starch/clay nanocomposites. *Journal of Materials Science*, *38*(5), 909–915.

Park, H. M, Li, X., Jin, C. Z., Park, C. Y., Cho, W. J., & Ha, C. S. (2002). Preparation and properties of biodegradable thermoplastic starch/clay hybrids. *Macromolecular Materials and Engineering*, *287*(8), 553–558.

Pascu, M. C., Popescu, M. C., & Vasile, C. (2008). Surface modifications of some nanocomposites containing starch. *Journal of Physics D: Applied Physics*, *41*(17), 175407.

Perera, C., & Hoover, R. (1999). Influence of hydroxypropylation on retrogradation properties of native, defatted and heat-moisture treated potato starches. *Food Chemistry*, *64*(3), 361–375.

Poutanen, K., & Forssell, P. (1996). Modification of starch properties with plasticizers. *Trends in Polymer Science*, *4*(4), 128–132.

Shogren, R. L. (1992). Effect of moisture content on the melting and subsequent physical aging of cornstarch. *Carbohydrate Polymers*, *19*(2), 83–90.

van Soest, J. J. G., Hulleman, S. H. D., de Wit, D., & Vliegenthart, J. F. G. (1996). Crystallinity in starch bioplastics. *Industrial Crops and Products*, *5*(1), 11–22.

Wilhelm, H. M., Sierakowski, M. R., Souza, G. P., & Wypych, F. (2003a). The influence of layered compounds on the properties of starch/layered compound composites. *Polymer International*, *52*(6), 1035–1044.

Wilhelm, H. M., Sierakowski, M. R., Souza, G. P., & Wypych, F. (2003b). Starch films reinforced with mineral clay. *Carbohydrate Polymers*, *52*(2), 101–110.

Yu, L., & Christie, G. (2001). Measurement of starch thermal transitions using differential scanning calorimetry. *Carbohydrate Polymers*, *46*(2), 179–184.

Zhang, X. Q., Dean, K., & Burgar, I. M. (2010). A high-resolution solid-state NMR study on starch–clay nanocomposites and the effect of aging on clay dispersion. *Polymer Journal*, *42*(8), 689–695.